ARM Cloud and Radiation at EPCAPE

Dan Lubin
Scripps Institution of Oceanography

EPCAPE Breakout Session
US Department of Energy 2022 ARM/ASR PI Meeting
24 October 2022

- California coastal clouds are well-studied going back nearly 100 years.
  - As early as 1923, related to emerging naval aviation based in San Diego, including as early as 1926 at Scripps Oceanography (Kloesel, 1992, *BAMS*).
- California marine stratocumulus were among the first cloud systems to be studied in the context of satellite remote sensing and global climate modeling improvement
  - First International Satellite Cloud Climatology Project (ISCCP) Regional Experiment (FIRE; Cox et al., 1987, *BAMS*; Albrecht et al., 1988, *BAMS*).
- Marine Stratus Radiation, Aerosol and Drizzle (MASRAD) is the first AMF deployment using state-of-the-art atmospheric and climate science equipment (Miller et al., 2005, *DOE/ER-ARM-0501*).
- Several aircraft campaigns focusing on ACI now have their data compiled in a unified database (Sorooshian et al., 2018, *Scientific Data*).

First Use of an Airplane for Atmospheric Research

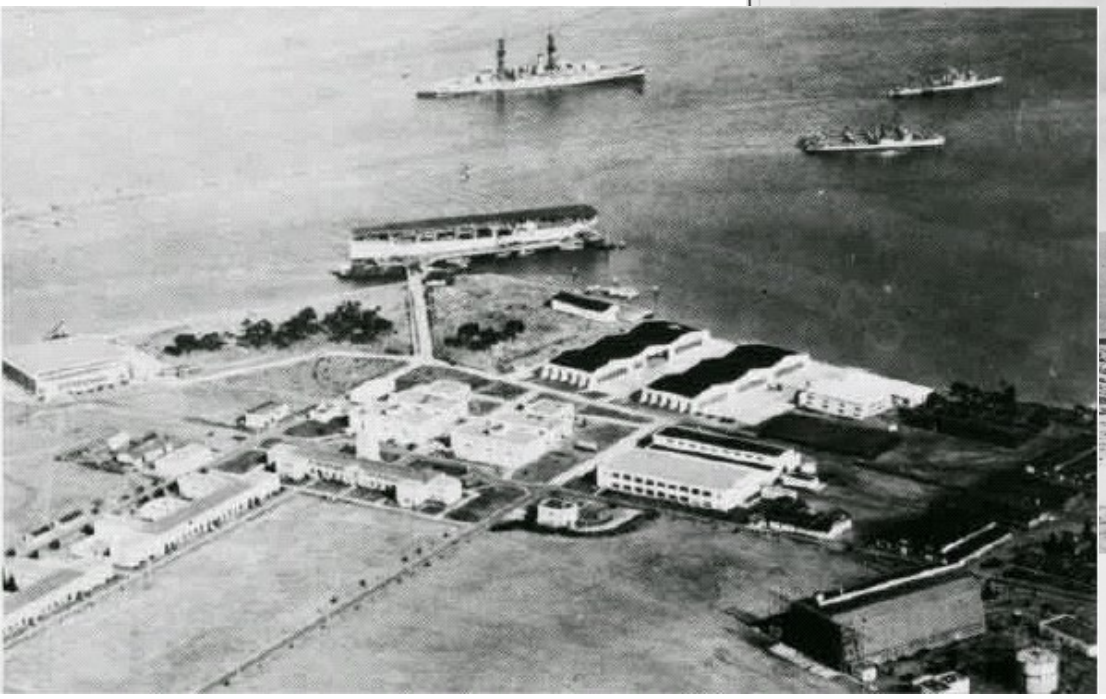

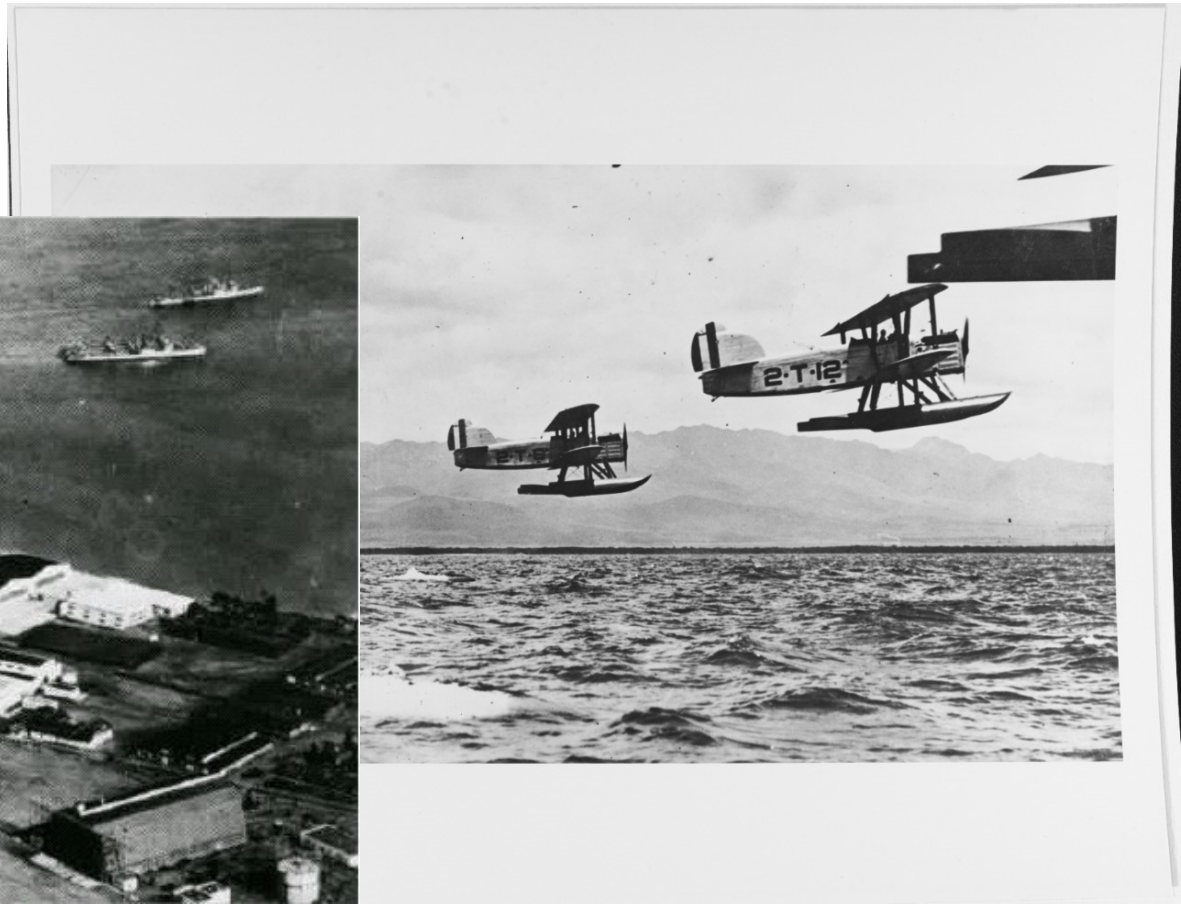

- Aircraft from US Naval Air Fleet, San Diego CA, 10 September 1923
- Pilot carrying “aerograph” to measure temperature, pressure and humidity, in his lap.
- Studied the marine stratocumulus layer, called the “Velo” in those days.

Coincidence? The Point Honda Disaster

8 September 1923

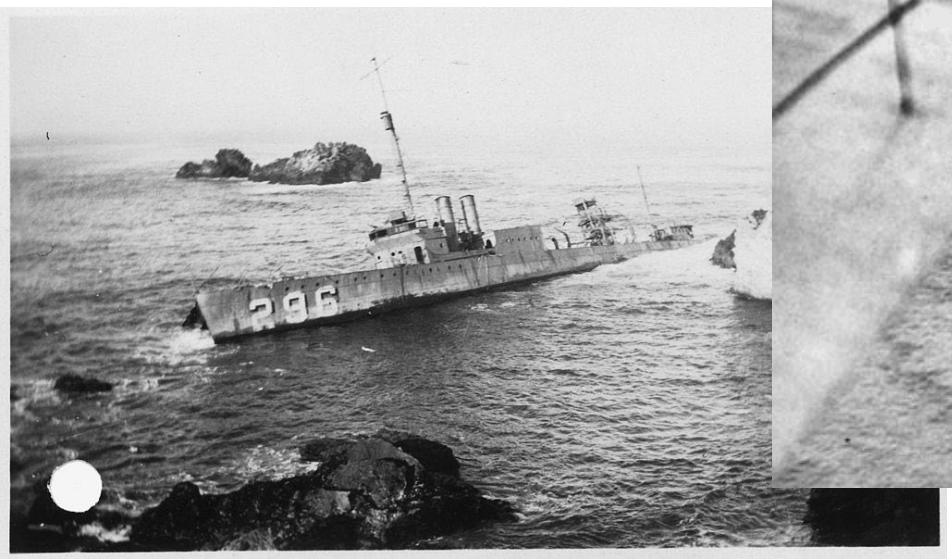

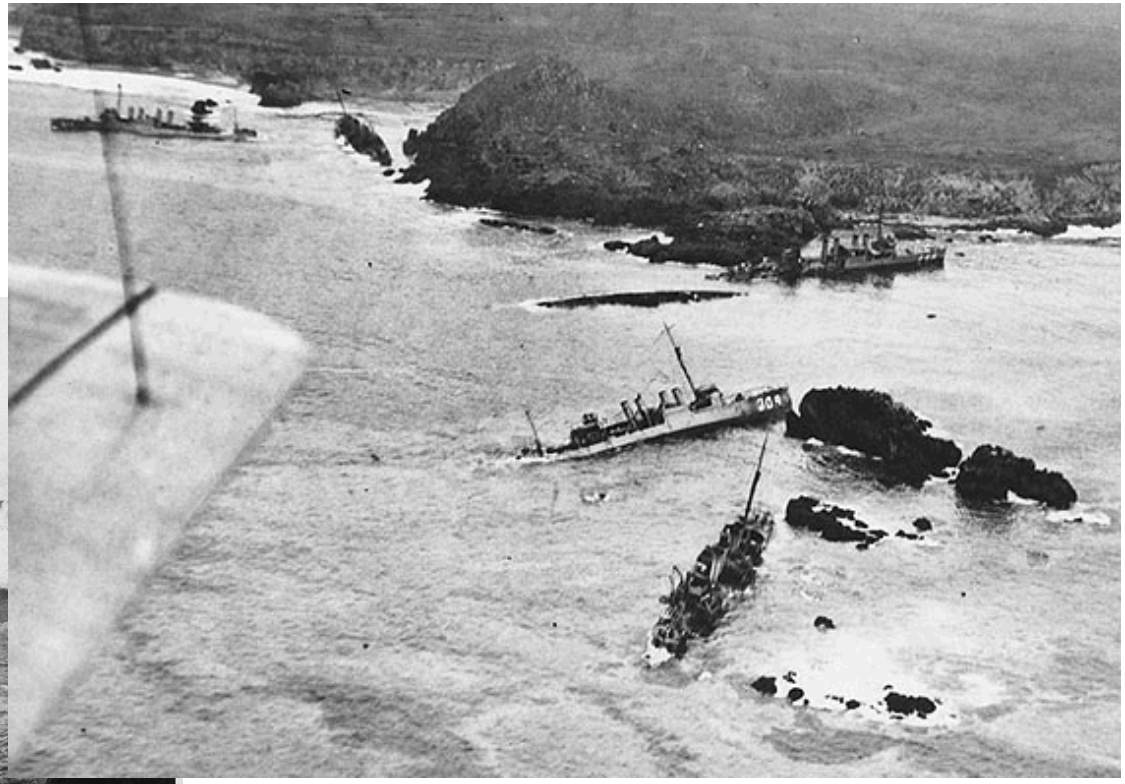

- Thirteen destroyers from DESRON 11 sailing from San Francisco to San Diego, participating in tactical and gunnery exercises.
- Poor visibility in fog, and currents stronger than normal, lead to seven being wrecked on the rocks at Point Honda, while proceeding full speed ahead at 20 knots. Loss of 23 sailors.

Climatology of California Coastal Stratiform Clouds

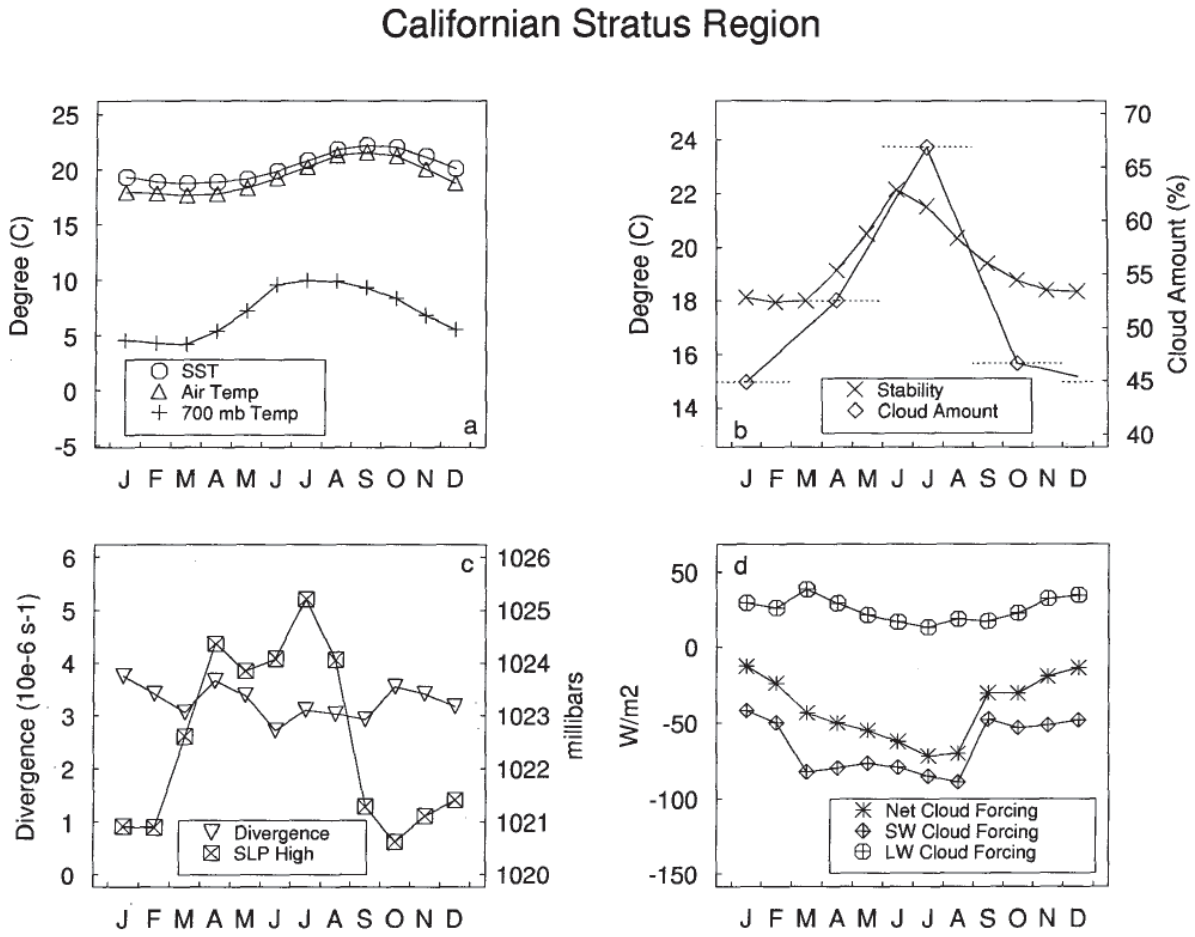

(a) temperatures, (b) lower troposphere stability (LTS) and stratus cloud amount,
(c) large-scale divergence of surface winds & peak SLP of N. Pacific subtropical high,
(d) ERBE-measured cloud forcing (Klein & Hartmann, 1993, *J. Climate*).

Early FIRE I Results

Duynkerke & Teixeira, 2001, *J. Climate*

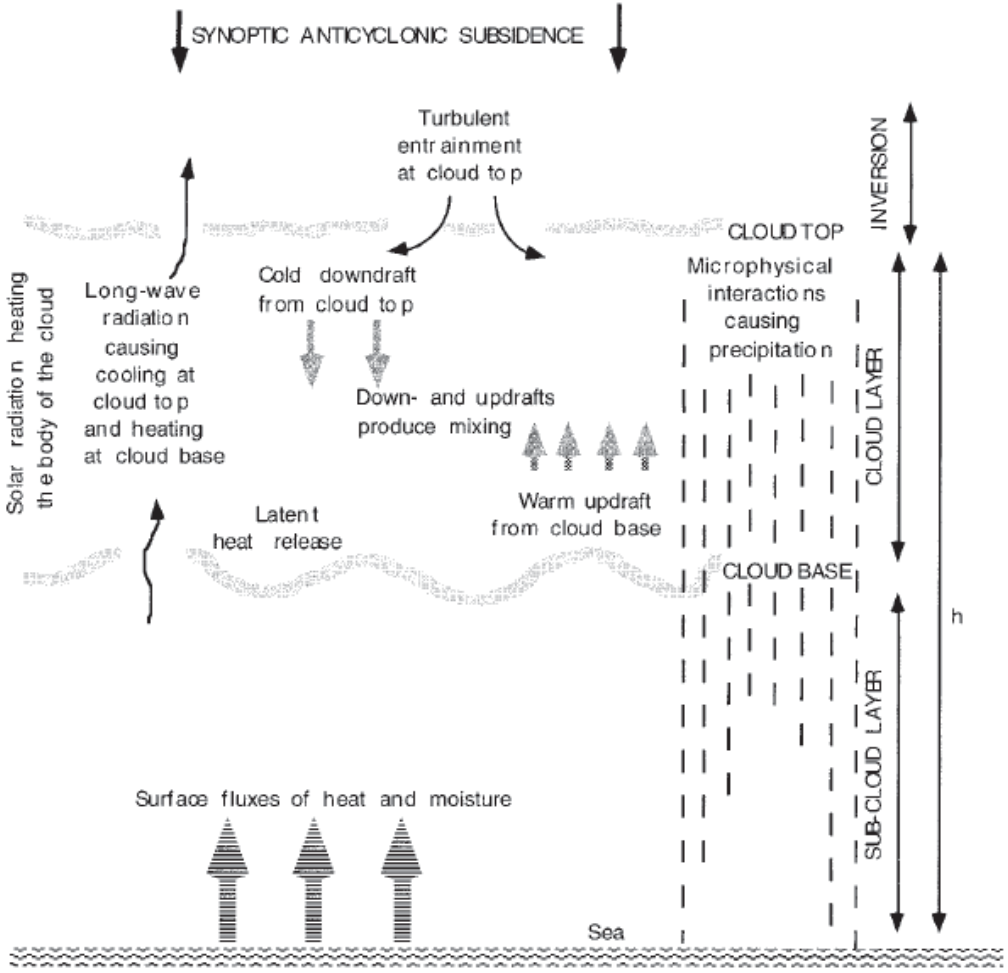

Schematic of important formation processes

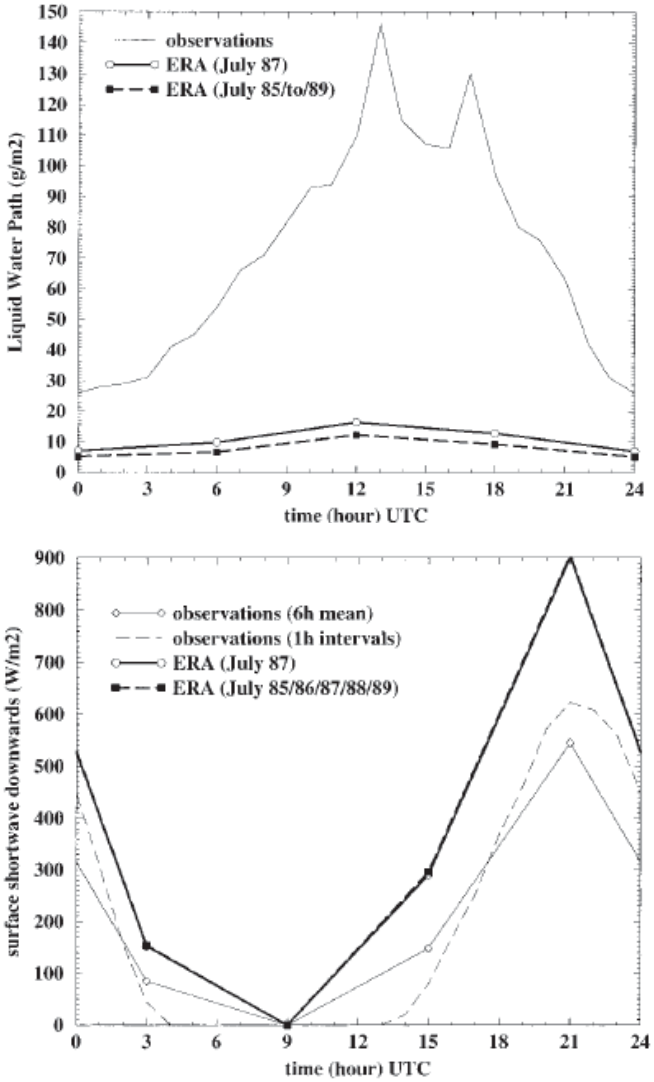

Diurnal variation in LWP and SW flux

Satellite-Observed Diurnal Variation

Greenwald & Christopher, 1999, *GRL*

Analyzing amplitude and phase of first harmonic of Fourier time series:

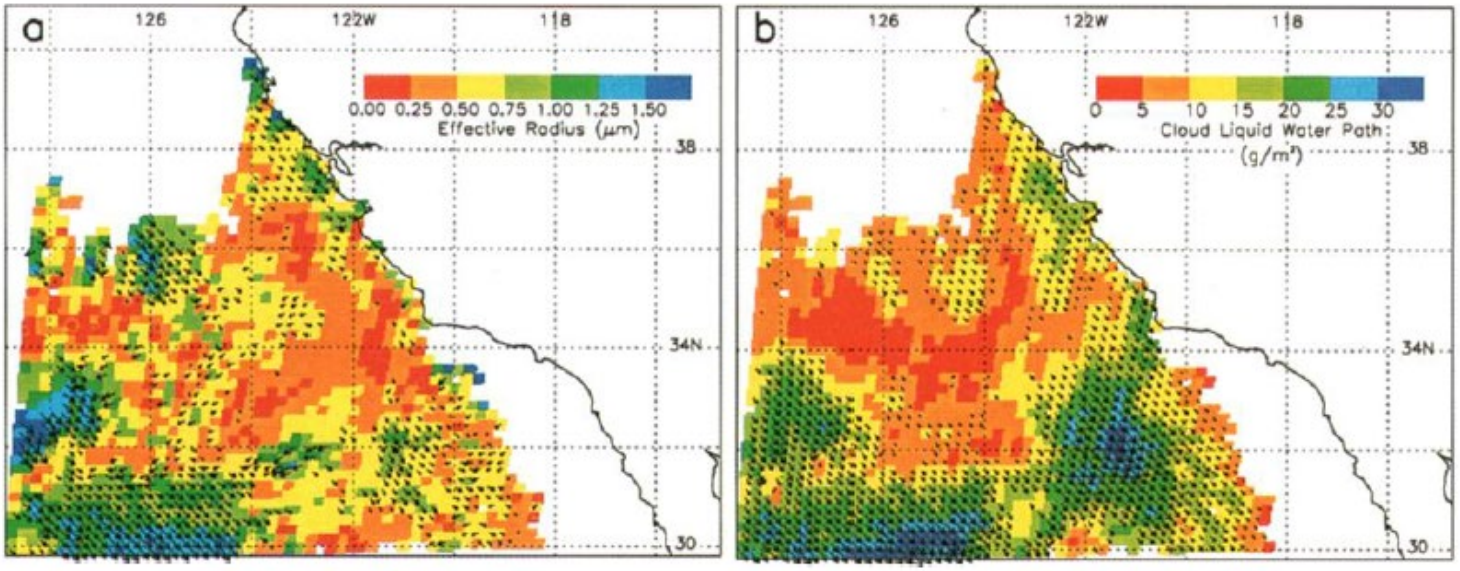

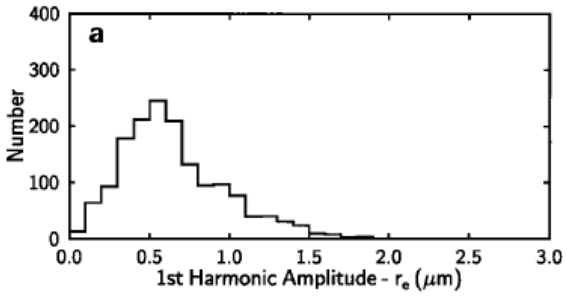

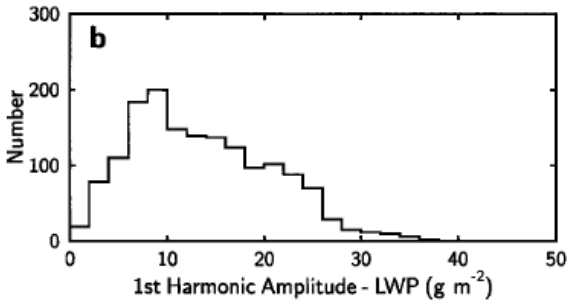

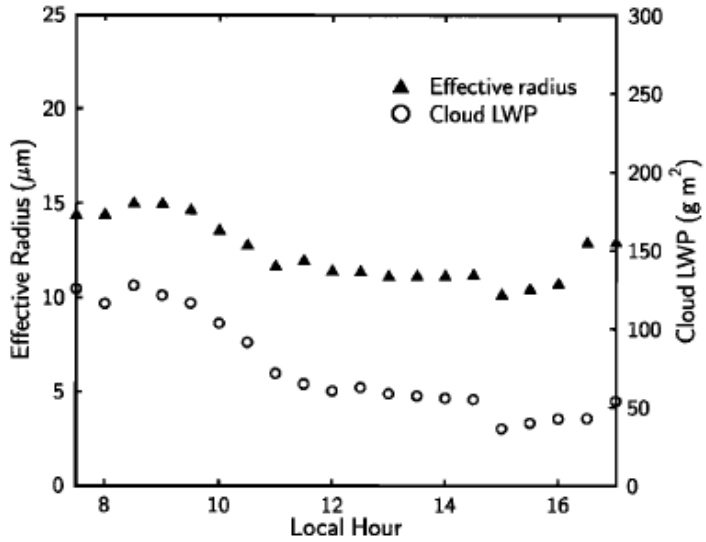

- Diurnal variation in both effective droplet radius r_e and liquid water path (LWP) is a spatially variable but consistent feature.

Variability in Optical Depth and Effective Droplet Radius

Szczodrak et al., 2001, *J. Atmos. Sci.*

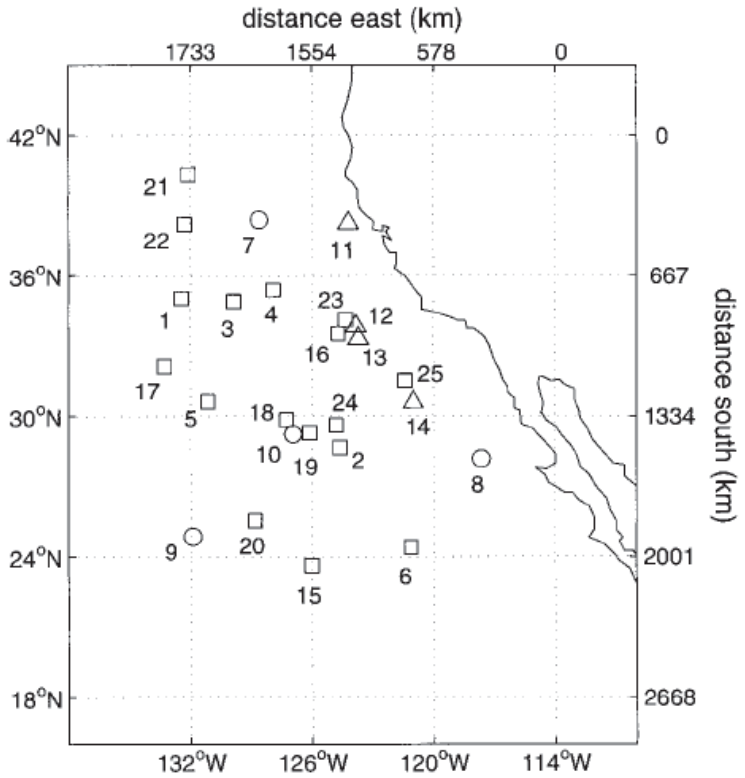

FIG. 1. The geographical location of 25 northeastern Pacific scenes used in section 4. Markers used for each scene are explained in more detail in section 4. □: scenes where for which $\tau \propto r_{eff}$; ○: scenes with bimodal distribution of N_{sat} (see section 4 for the definition); △: scenes with thick clouds.

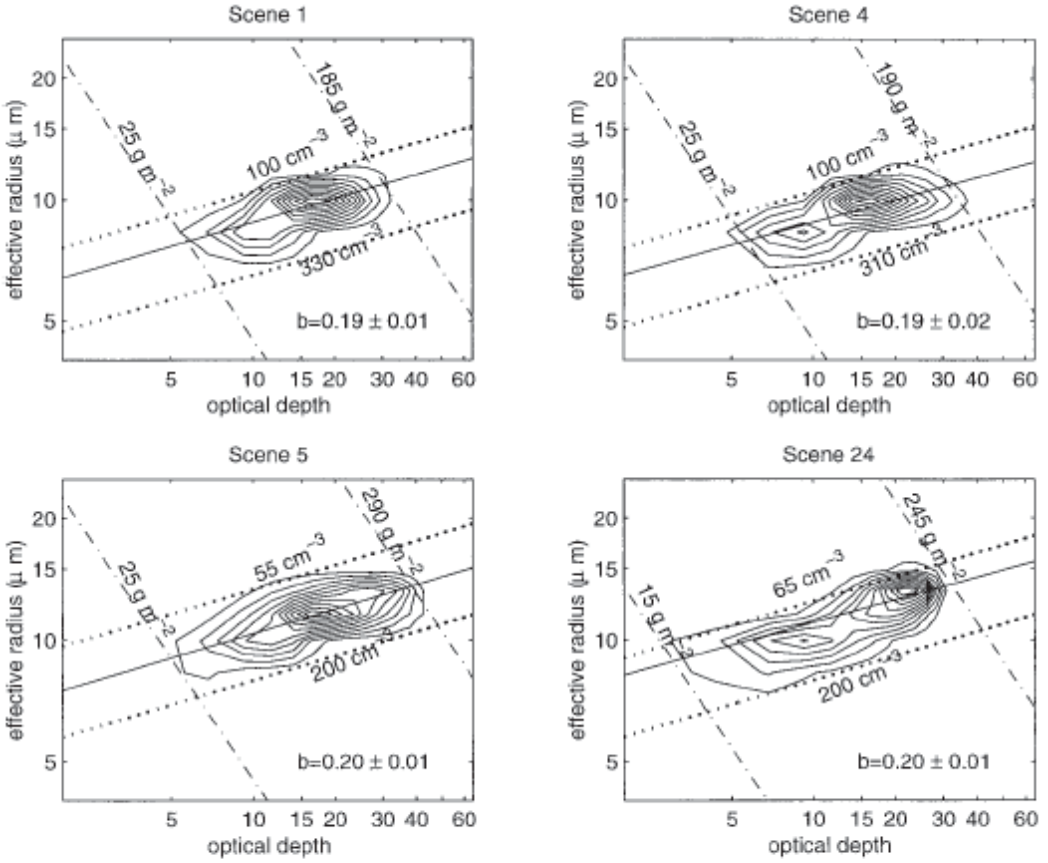

FIG. 2. Log–log contour plots of r_{eff} and τ from four cloudy scenes. The contours are of the frequency density η, where $\eta \Delta \log\tau \Delta \log r_{eff}$ denotes the number of pixels with optical depth and effective radii in the range ($\log\tau < \log\tau' < \log\tau + \Delta \log\tau$; $\log r_{eff} < \log r'_{eff} < \log r_{eff} + \Delta \log r_{eff}$). The dot–dashed, labeled lines are isolines of lwp given by (3c); the dotted labeled lines are isolines of N_{sat} given by (3b). Also shown on each panel is the linear least squares regression line (solid), with the slope b and its uncertainty. Clouds with both high (τ, r_{eff}) correlations and $b \sim 0.2$ are denoted by a □ in Fig. 1.

- In majority of thinner layers, $r_e \alpha \tau^{1/5}$

Early Work With Ship Tracks Near Southern California Coast

King et al., 1993, *J. Geophys. Res.*

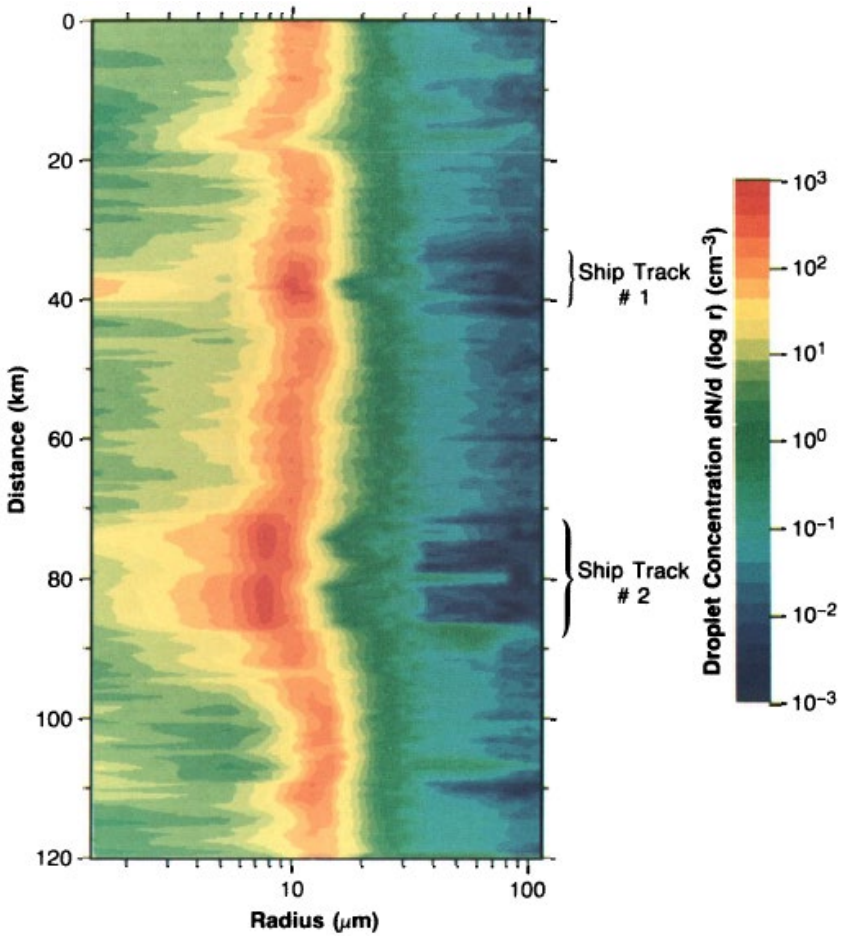

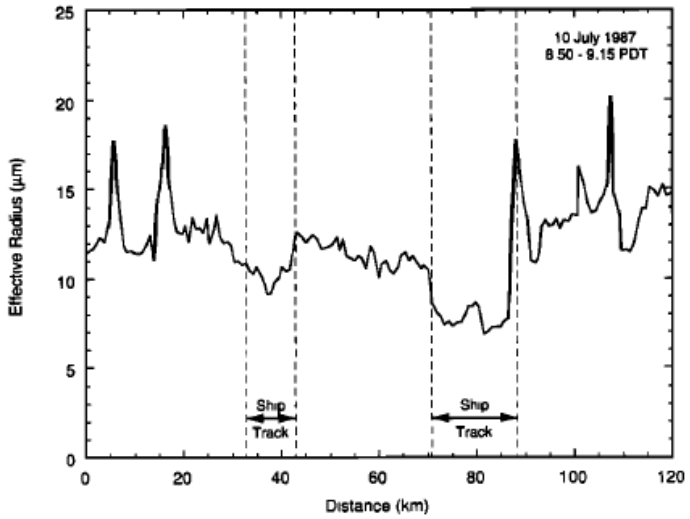

Effective radius

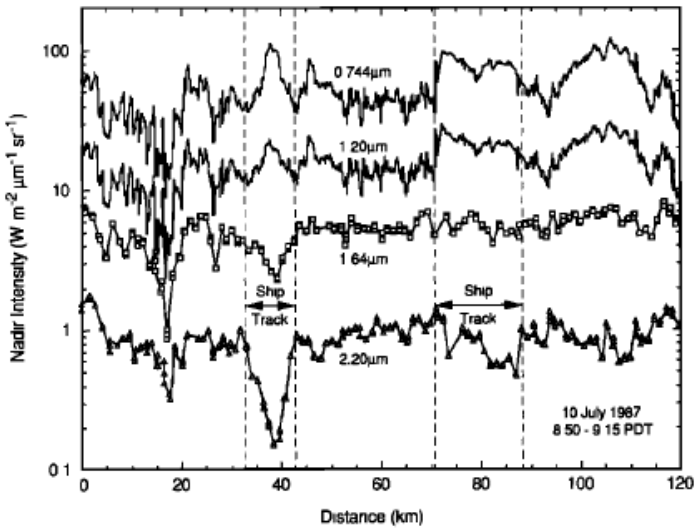

Multispectral nadir-viewing radiance

MASRAD-Based ACI Study

McComiskey et al., 2009, *J. Geophys. Res.*

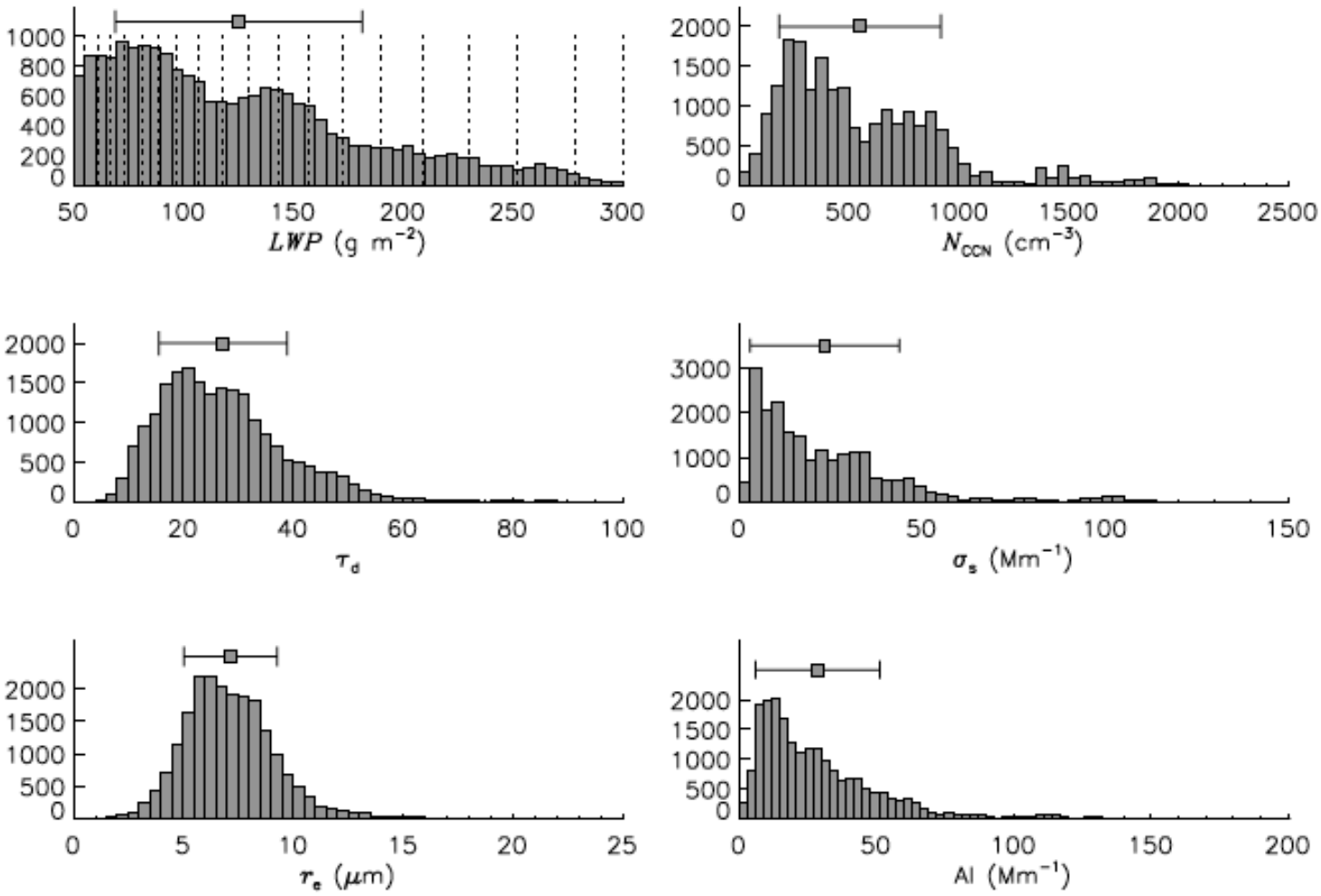

Figure 2. Histograms of observed aerosol and cloud properties over the Pt. Reyes deployment. The square symbols above the histograms represent the mean, and the bars represent one standard deviation from the mean.

MASRAD-Based ACI Study

McComiskey et al., 2009, *J. Geophys. Res.*

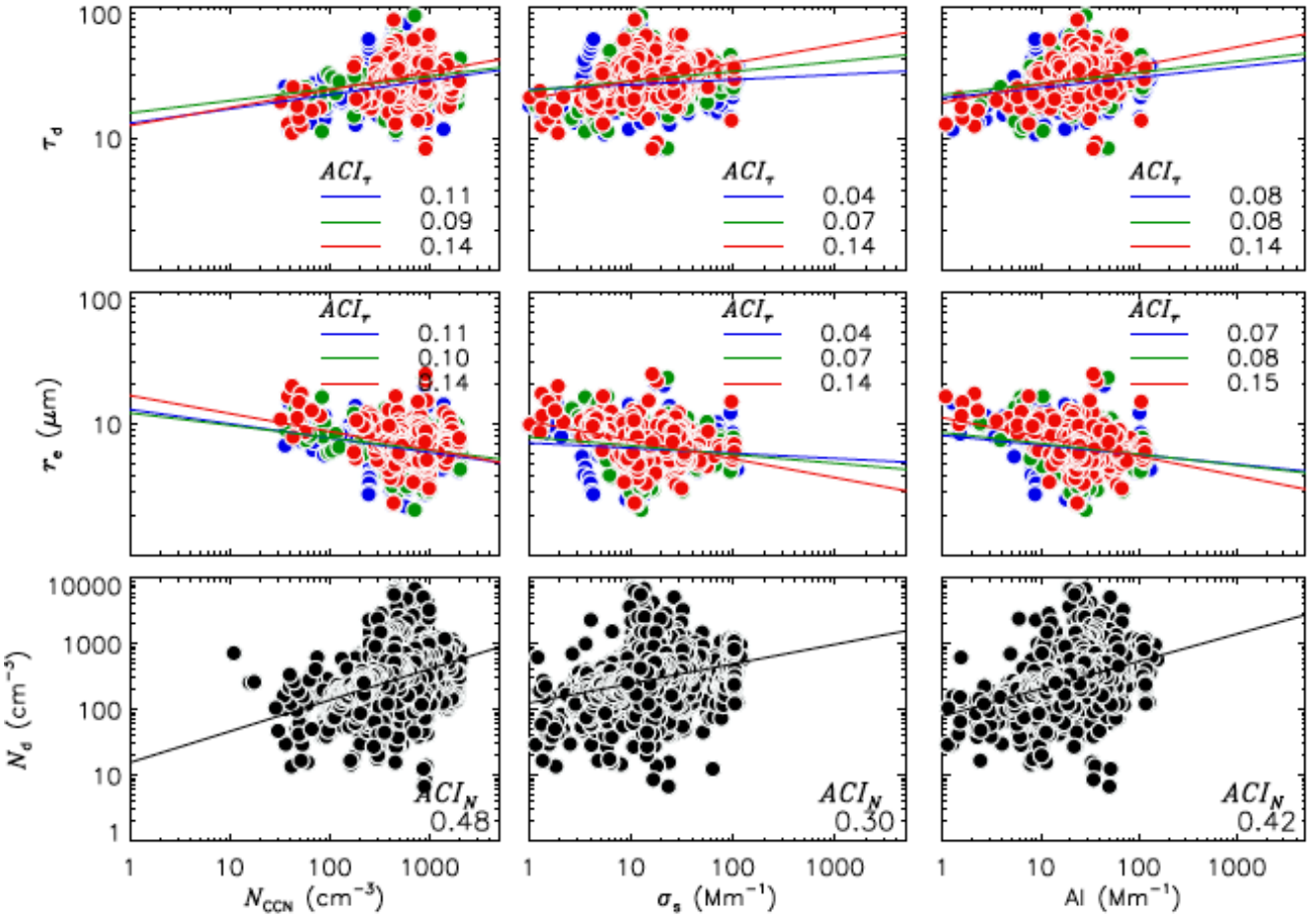

Figure 3. Measures of ACI from equation (1) sorted by LWP and showing expected consistency among the different measures. Cloud properties (τ_d, r_e, N_d) are derived from measurements made by the 2NFOV and MWR instruments, and aerosol properties (N_{CCN}, σ_s, AI) are derived from ground-based in situ observations made by the Aerosol Observation System (AOS). Regressions are made for LWP bins geometrically increasing in size by 10% around an approximate mean LWP value (120 g m^{-2}) for the deployment. Regressions shown are for the following bins: blue, 107 $\leq$ LWP $<$ 118 g m^{-2}; green, 118 $\leq$ LWP $<$ 130 g m^{-2}; and red, 130 $\leq$ LWP $<$ 143 g m^{-2}.

Space-Time Propagation in Summer Coastal California Clouds

Clemesha et al., 2016, *Geophys. Res. Lett.*

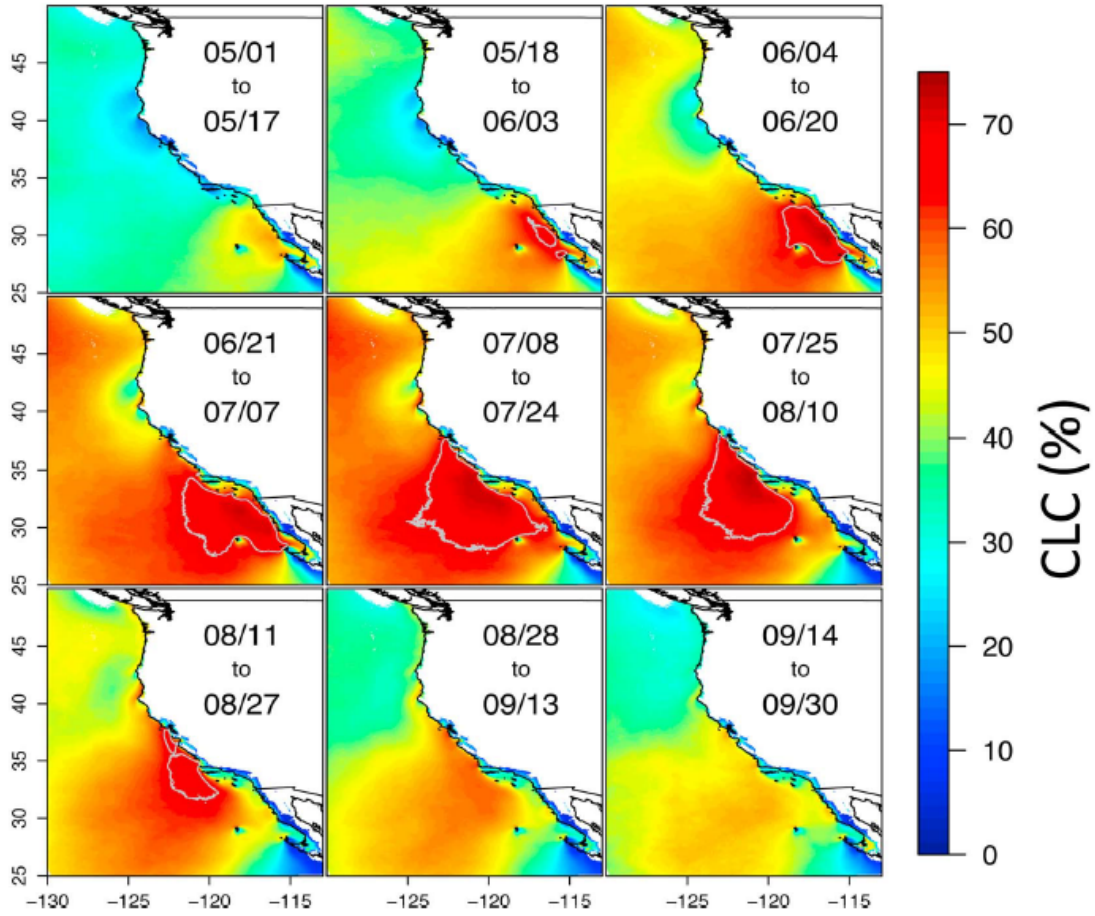

Figure 2. The 17 day averages of CLC seasonal cycle. Gray contour denotes 65% CLC (the domain-wide 95th percentile of CLC).

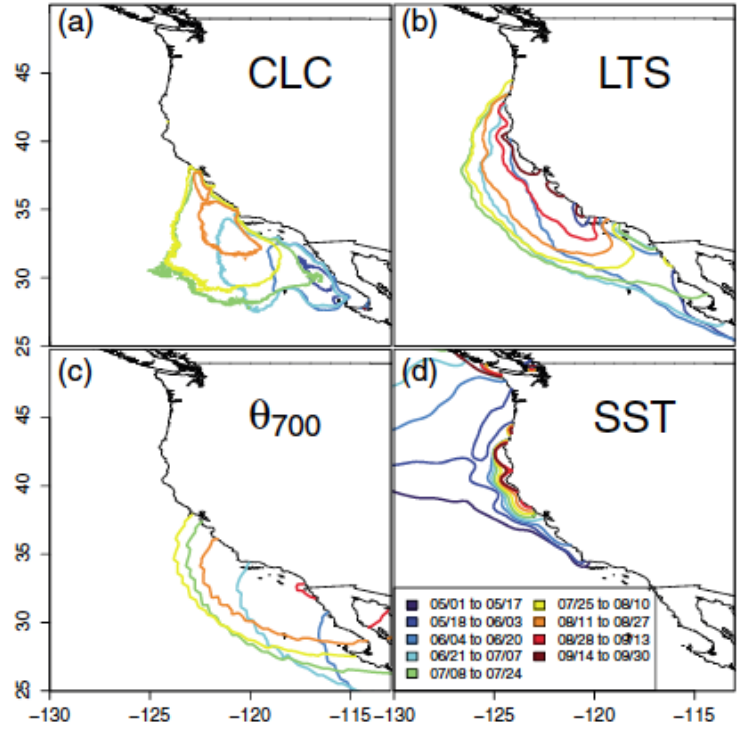

Figure 3. The 95th percentile contours of (a) CLC (65%), (b) LTS (23.7°C), and (c) θ_{700} (41.4°C) and the 10th percentile contours for (d) SST (12.8°C) for 17 day periods (colors).

Urbanization Influences on Coastal California Cloud Properties

Williams et al., 2015, *GRL*

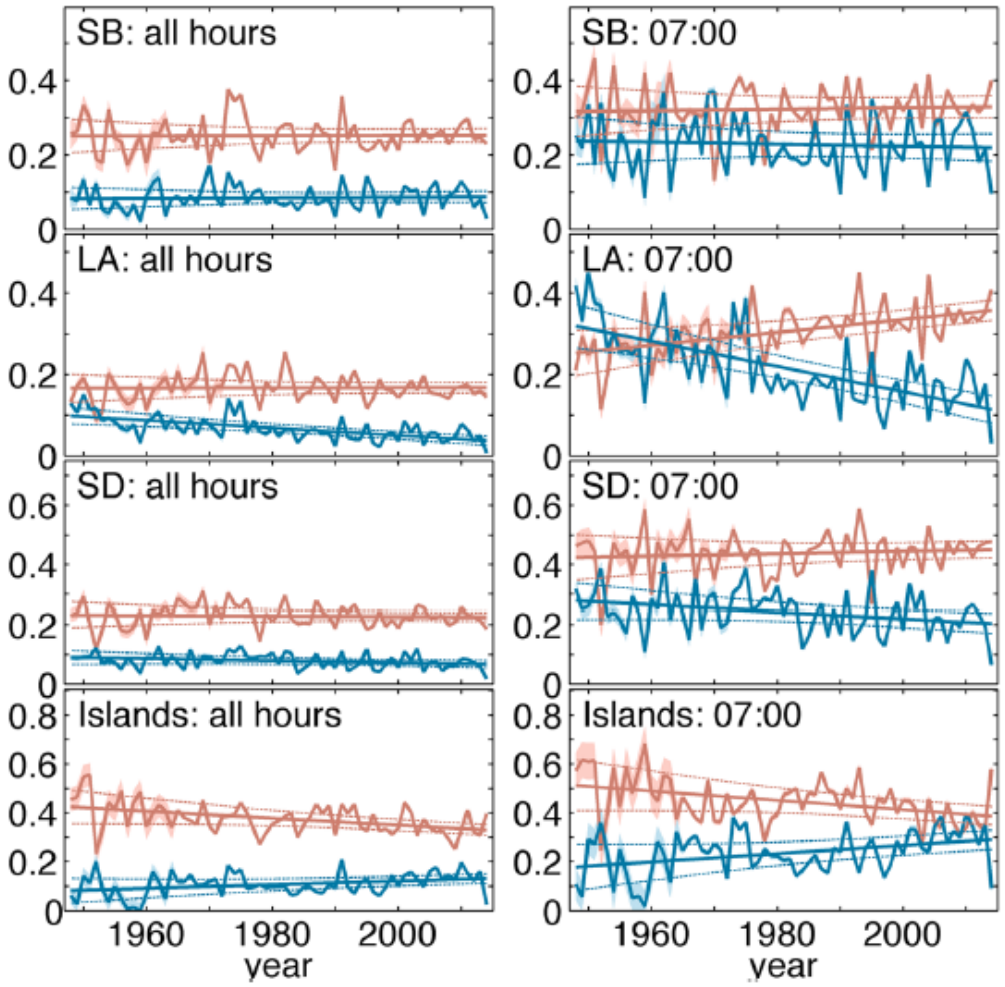

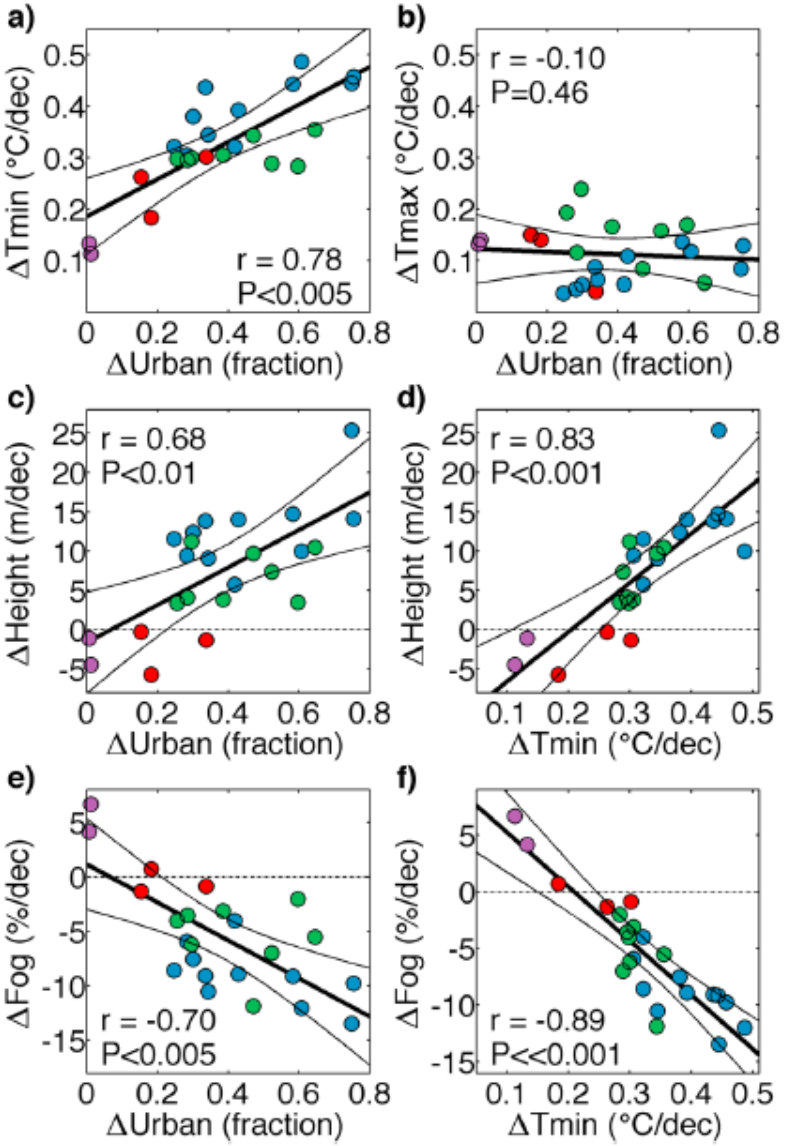

Coastal California Cloud Influences on Heat Waves

Clemesha et al., 2018, *Clim. Dyn.*

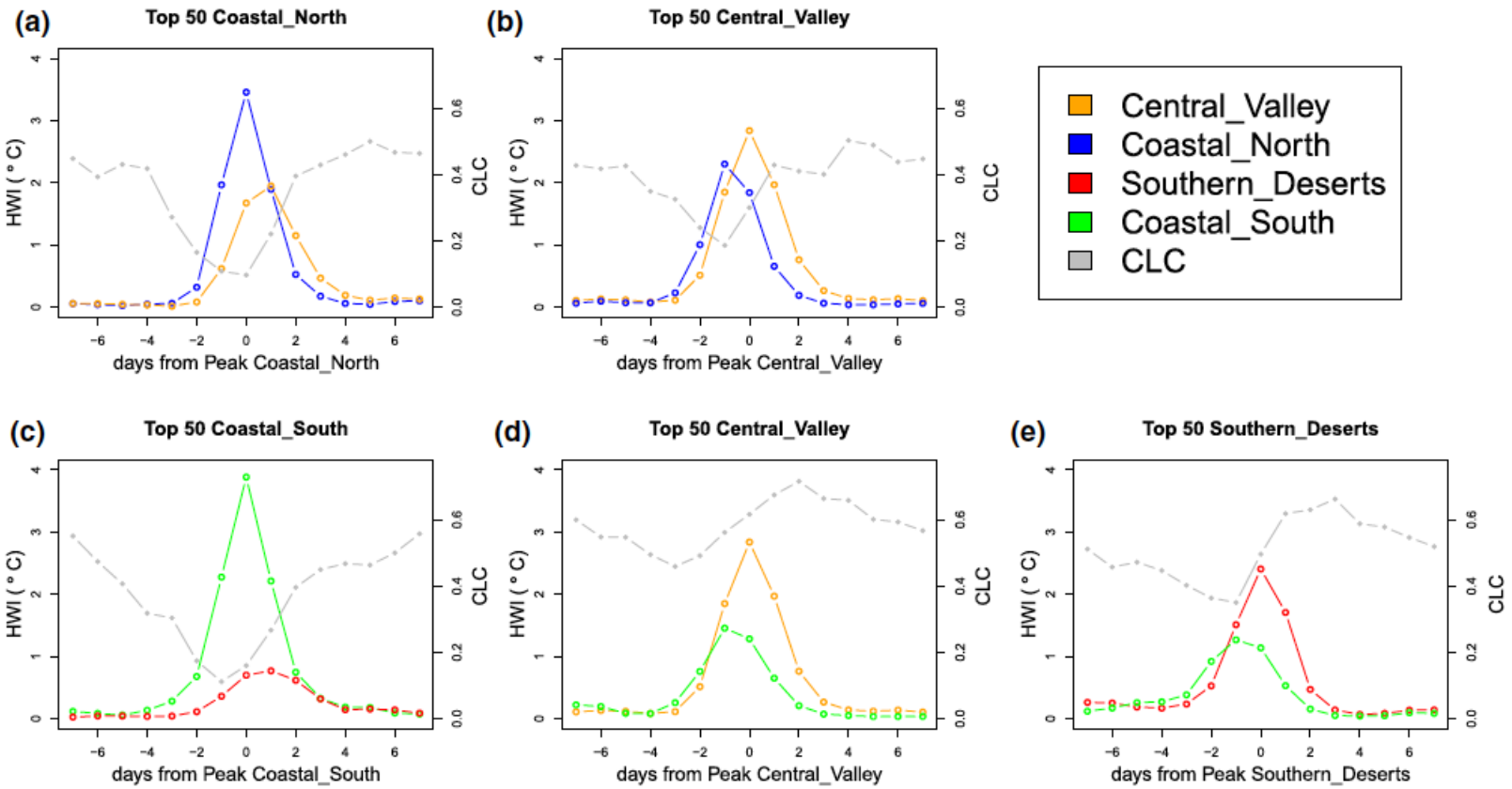

Fig. 5 HWI composites of top 50 focus region heat waves with other paired region shown and CLC for coastal region (*gray trace*). Paired regions are denoted as "focus region–paired region" **a** "Coastal North–Central Valley", **b** "Central Valley–Coastal North", **c** "Coastal South–Southern Deserts", **d** "Central Valley–Coastal South", **e** "Southern Deserts–Coastal South". This ordering is used for all following five *panel* figures